Reaction of 2,2′-Bipyridine (bpy) with Dirhodium Carboxylates: Mono-bpy Products with Variable Chelate Binding Modes and Insights into the Reaction Mechanism

Charles A. Crawford,† John H. Matonic,‡ William E. Streib,† John C. Huffman,† Kim R. Dunbar,*,‡ and George Christou*,†

Department of Chemistry and Molecular Structure Center, Indiana University, Bloomington, Indiana 47405, and Department of Chemistry, Michigan State University, East Lansing, Michigan 48824

Received December 2, 1992

Synthetic procedures are described for the preparation of mono-2,2′-bipyridine (bpy) complexes possessing the Rh_2^{4+} core. Reaction of $Rh_2(OAc)_4(MeOH)_2$ (**1**) with 1 equiv of bpy in Me_2CO produces $Rh_2(OAc)_4(bpy)$ (**3**) in excellent yield. The compound crystallizes in the triclinic space group $P\bar{1}$ with the following cell parameters at −172 °C: a = 9.883(3), b = 13.078(5), c = 8.323(2) Å; α = 97.02(2), β = 106.90(1), γ = 94.29(2)°; Z = 2; V = 1015 Å^3. The structure was solved by direct methods (MULTAN) and refined to values of conventional indices R (R_w) of 4.72% (4.50%) using 2636 unique reflections with $F_o > 3\sigma(F_o)$. The two Rh^{2+} centers are bridged by three η^1:η^1:μ_2 AcO^- groups over a Rh–Rh bond distance of 2.475(2) Å. The coordination spheres of Rh(1) and Rh(2) are completed by chelating bpy and OAc^- groups, respectively. The chelating OAc^- is asymmetrically bound as a consequence of the axial/equatorial positioning of its two oxygen atoms O(27) and O(29). Compound **3** undergoes a reaction on dissolution in MeOH to give $[Rh_2(OAc)_3(bpy)(MeOH)](OAc)\cdot 2MeOH$ (**4**) as determined by ^1H NMR (1D- and 2D-homonuclear J-resolved spectroscopy), elemental analysis, conductivity measurements, and reactivity studies. Reaction of $Rh_2(O_2CCF_3)_4(Me_2CO)_2$ (**2**) with 1 equiv of bpy in CH_2Cl_2, followed by recrystallization of the product from THF/H_2O, produces crystals of $Rh_2(O_2CCF_3)_4(bpy)(THF)(H_2O)\cdot THF$ (**5**). Compound **5** crystallizes in the monoclinic space group Pc with the folowing cell parameters at −105 °C: a = 10.683(8), b = 9.170(8), c = 17.783(1) Å; α = 90.00, β = 103.52(7), γ = 90.00°; Z = 2, V = 1693 Å.^{3} The structure was solved by direct methods (MITHRIL) and refined to values of R (R_w) of 5.1% (5.8%) using 2493 unique reflections with $F > 3\sigma(F)$. The two Rh^{2+} centers are bridged by two η^1:η^1:μ_2 $O_2CCF_3^-$ ligands across a Rh–Rh separation of 2.520(3) Å. Coordination about Rh(1) is completed by two terminal η^1-$O_2CCF_3^-$ groups in equatorial sites with the axial site being occupied by a water molecule. Rh(2) is ligated by a chelating bpy group in the equatorial plane, with axial ligation being provided by a THF molecule. Reaction mixtures comprising $[Rh_2(OAc)_2(MeCN)_6](BF_4)_2$ (**6**) and 1 equiv of bpy in MeCN lead to isolation of $[Rh_2(OAc)_2(bpy)(MeCN)_4](BF_4)_2\cdot MeCN$ (**7**). Compound **7** crystallizes in the triclinic space group $P\bar{1}$ with the following cell parameters at −170 °C: a = 12.381(2), b = 14.301(2), c = 12.246(2) Å; α = 94.60(1), β = 105.84(1), γ = 117.42(1)°; Z = 2; V = 1797 Å^3. The structure was solved by direct methods (MULTAN) and refined to values of R (R_w) of 4.92% (5.74%) using 4723 unique reflections with $F > 3\sigma(F)$. The two metals are bridged by two *cis* η^1:η^1:μ_2-OAc^- groups that span a Rh–Rh distance of 2.5395(8) Å. Coordination at Rh(1) is completed by a chelating bpy in the equatorial plane and an axial MeCN ligand, while the coordination sphere of Rh(2) is completed by two equatorial MeCN molecules and an axial MeCN molecule.

Downloaded via UNIV OF TEXAS SAN ANTONIO on October 23, 2024 at 20:58:41 (UTC).
See https://pubs.acs.org/sharingguidelines for options on how to legitimately share published articles.

Introduction

Dirhodium tetracarboxylates exhibit extensive carcinostatic activity against a wide variety of tumors in mice.[1] This has stimulated intense study, by a number of groups, of the chemistry of rhodium carboxylates with ligands of relevance to this area.[2–4] These rhodium complexes have been shown to significantly inhibit RNA and DNA synthesis *in vivo*, with DNA synthesis being affected to a much larger degree.[1] This is believed to be the result of $Rh_2(O_2CR)_4$ compounds binding to the single-stranded template present in DNA synthesis that is not present in RNA synthesis since RNA polymerase acts upon duplex templates.[1c,d] Studies also indicate that rhodium(II) carboxylates bind preferentially to adenine nucleobases in single-stranded DNA.[1c,d] The higher affinity of $Rh_2(O_2CR)_4$ compounds for adenine residues may result from interligand hydrogen bonding as seen in the cobalt-containing species $[Co(acac)_2(NO_2)(ado)]$ (acac = acetylacetonate, ado = adenosine).[5,6] Purine ligands containing exocyclic amino substituents, as found in adenine derivatives, are expected to favor those metal complexes containing oxygen donor ligands; the metal–purine interaction would be expected to form through lone-pair donation by the N(7) of adenine residues into the labile axial site of the rhodium dimer, with this interaction

† Indiana University.
‡ Michigan State University.

(1) (a) Hughes, R. G., Jr.; Bear, J. L.; Kimball, A. P. *Proc. Am. Assoc. Cancer Res.* **1972**, *13*, 120. (b) Erck, L.; Rainen, L.; Whileyman, J.; Chang, I.-M.; Kimball, A. P.; Bear, J. L. *Proc. Soc. Exp. Biol. Med.* **1974**, *145*, 1278. (c) Bear, J. L.; Gray, H. B.; Rainen, L.; Chang, I.-M.; Howard, R.; Serio, G.; Kimball, A. P. *Cancer Chemother. Rep.* **1975**, *59*, 611. (d) Erck, A.; Sherwood, E.; Bear, J. L.; Kimball, A. P. *Cancer Res.* **1976**, *36*, 2204. (e) Tselepi-Kalouli, E.; Katsaros, N. *J. Inorg. Biochem.* **1990**, *40*, 95. (f) Bear, J. L.; Howard, R. A.; Dennis, A. M. *Curr. Chemother.* **1978**, 1321. (g) Howard, R. A.; Kimball, A. P.; Bear, J. L. *Cancer Res.* **1979**, *39*, 2568.
(2) (a) Goodgame, D. M. L.; Page, C. J.; Williams, D. J. *Inorg. Chim. Acta* **1988**, *153*, 219. (b) Goodgame, D. M. L.; O'Mahoney, C. A.; Page, C. J.; Williams, D. J. *Inorg. Chim. Acta* **1990**, *175*, 141. (c) Dyson, T. M.; Morrison, E. C.; Tocher, D. A.; Dale, L. D.; Edwards, D. I. *Inorg. Chim. Acta* **1990**, *169*, 127. (d) Nothenberg, M. S.; Takeda, G. K. F.; Najjar, R. *J. Inorg. Biochem.* **1991**, *42*, 217.
(3) (a) Farrell, N.; Vargas, M. D.; Mascarenhas, Y. A.; Gambardella, M. T. P. *Inorg. Chem.* **1987**, *26*, 1426. (b) Farrell, N. *J. Inorg. Biochem.* **1981**, *14*, 261. (c) Farrell, N. *J. Chem. Soc., Chem. Commun.* **1980**, 1014.
(4) (a) Pneumatikakis, G.; Hadjiliadis, N. *J. Chem. Soc., Dalton Trans.* **1979**, 596. (b) Aoki, K.; Yamazaki, H. *J. Am. Chem. Soc.* **1984**, *106*, 3691. (c) Aoki, K.; Yamazaki, H. *J. Chem. Soc., Chem. Commun.* **1980**, 186.
(5) Marzilli, L. G. *Prog. Inorg. Chem.* **1977**, *23*, 255.
(6) Sorrel, T.; Epps, L. A.; Kirstennacher, T. G.; Marzilli, L. G. *J. Am. Chem. Soc.* **1977**, *99*, 2173.

0020-1669/93/1332-3125$04.00/0 © 1993 American Chemical Society

Pictiva EX2017
Samsung v Pictiva
IPR2024-01094

being augmented by hydrogen bonding between the free amino group and an equatorial carboxylate oxygen of the rhodium dimer.[5,6]

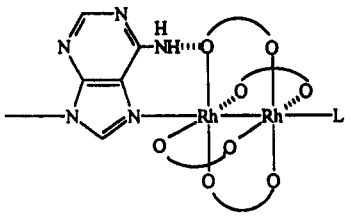

Such a system has recently been crystallographically confirmed in a rhodium dimer possessing axially-bound adenosine groups, *viz.* $Rh_2(OAc)_4(ado)_2$.[7] Although the above interaction with adenine groups is perhaps of importance to the biological activity of these dinuclear complexes, this has yet to be proven and the detailed mechanism of activity remains unknown. Recently, Lippard and co-workers structurally characterized the adduct formed between cisplatin, *cis*-$Pt(NH_3)_2Cl_2$, and a guanosine dinucleotide, d(pGpG).[8] Similarly, Reedijk and co-workers have obtained the crystal structure of the complex with the trinucleotide d(CpGpG).[9] These structures confirm unequivocally that binding of cisplatin to DNA can occur through two adjacent bases of the same strand, the two binding sites at the metal being the *cis* sites formerly occupied by the Cl^- atoms.[10] Such *cis* binding modes have also been proposed in the biological activity of certain metallocene derivatives (Cp_2MX_2; Cp = $C_5H_5^-$, M = Ti, Nb; X = halide)[11,12] though recent developments indicate that such mechanisms are inoperative where M = V[13] and Mo.[14] In the above systems, the d(GpG) unit acts as a *chelating* ligand to a single metal atom. In contrast, such a binding possibility has not been considered in the study of $Rh_2(O_2CR)_4$ activity since the two labile axial sites are at opposite ends of the molecule. It has thus been assumed that binding of $Rh_2(O_2CR)_4$ complexes to DNA can only occur to a single base or through long distance linkages, as postulated for *trans*-$(NH_3)_2PtCl_2$ which binds to nonadjacent nucleotides.[15] It is not clear, however, that this is a particularly safe assumption.

To explore the possibility that the Rh_2^{4+} core could indeed bind to DNA in a similar fashion to cisplatin, we have initiated a program directed toward the investigation of the interaction of this and other dinuclear cores with chelating nitrogen-donor ligands. These model systems are designed to establish possible *biological* binding modes. Previous reports of complexes comprising neutral nitrogen chelates bound to a Rh_2^{4+} core are few and include compounds of formula $[Rh_2(O_2CR)_2(N\text{-}N)_2L_2]^{n+}$, where N-N is dimethylglyoxime (L = PPh_3, n = 2),[16] phenanthroline (L = Cl^-, n = 0),[17] and 2,2′-bipyridine (L = Cl^-, n = 0).[18] In all of these compounds, two chelates are bound to the dinuclear unit in *syn* positions. Tri- and tetradentate derivatives of 1,8-naphthyridine have also been prepared in which a 1,8-naphthyridine fragment bridges the two metal atoms, with axial ligation provided by ligand substituents.[19] However, a search of the rhodium carboxylate literature has failed to locate an example of a Rh_2^{4+} complex possessing a *single* bidentate nitrogen chelate to mimic binding by two adjacent nucleobases. Also, it is clear that little study has been devoted to the ligand substitution reactions of $Rh_2(O_2CR)_4$ complexes with such nitrogen chelates, *vis-à-vis* mechanisms, intermediates, etc. We herein report the results of our study of the reactions between rhodium(II) carboxylates and 1 equiv of 2,2′-bipyridine, the latter representing our initial choice for a mimic of two adjacent DNA bases. Some initial results have already been briefly communicated.[20]

Experimental Section

Synthesis. All manipulations were performed under aerobic conditions unless otherwise noted. $RhCl_3{\cdot}3H_2O$ (Sigma) was used as received. 2,2′-Bipyridine (bpy) was recrystallized from $MeCN/H_2O$ and dried *in vacuo* prior to use. $Rh_2(OAc)_4(MeOH)_2$ (**1**)[21] and $[Rh_2(OAc)_2(MeCN)_6](BF_4)_2$ (**6**)[22] were prepared by literature procedures.

$Rh_2(O_2CCF_3)_4(Me_2CO)_2$ (2). This was prepared by the following modified version of the published procedure.[21] In a typical preparation, complex **1** (0.400 g) was refluxed in CF_3COOH (15 mL) for approximately 3 h. CF_3COOH was then removed by evaporation, the residue extracted into acetone (5 mL), and the product crystallized by addition of hexanes (20 mL). To ensure complete precipitation, the acetone was slowly evaporated leaving complex **2** to be filtered from hexanes. Yields were essentially quantitative (0.58 g, 94%).

$Rh_2(OAc)_4(bpy)$ (3). This preparation is a modification of a procedure reported earlier.[20] An aqua-blue slurry of **1** (30.3 mg, 60 μmol) in acetone (10 mL) was treated with solid bpy (9.4 mg, 60 μmol) and stirred at room temperature for 24 h to give an olive-green precipitate of **3**. The solid was isolated by filtration, washed copiously with acetone, and dried *in vacuo*. The yield was 34.0 mg, 95%. Anal. Calcd for $C_{18}H_{20}N_2O_8Rh_2$: C, 36.14; H, 3.37; N, 4.68. Found: C, 36.29; H, 3.41; N, 4.65. ^{1}H NMR in CD_2Cl_2 (ppm): O_2CCH_3, 2.175 (s, 3), 2.149 (s, 3), 1.691 (s, 6); bpy, 9.654 (d, 1), 9.410 (d, 1), 8.359 (d, 1), 8.288 (d, 1), 8.241 (d, 1), 7.968 (t, 1), 7.875 (t, 1), 7.471 (t, 1). Electronic spectrum in CH_2Cl_2 [λ_{max}/nm (ϵ_M/L mol^{-1} cm^{-1})]: 609 (350), 446 (2110), 426 (2005), 300 (19 085), 276 (20 760), 244 (16 710). Solid-state reflectance UV/vis (λ_{max}/nm): 420, 594. IR data (KBr pellet, cm^{-1}): 3319 (m), 3034 (m), 1580 (s), 1563 (s), 1456 (s), 1424 (s), 1406 (s), 774 (m), 708 (m), 689 (m).

$[Rh_2(OAc)_3(bpy)(MeOH)_3](OAc)$ (4). An olive green suspension of **3** (100 mg, 0.167 mmol) in MeOH (10 mL) was stirred for 24 h at room temperature to give an emerald green solution. Addition of Et_2O (25 mL) to the MeOH solution gave a green precipitate of **4**, which was isolated by filtration, washed with Et_2O, and dried in air. The yield was 95.1 mg, 82%. A sample dried under vacuum for analytical purposes lost the axial MeOH molecules and was hygroscopic; the analytical data were consistent with $[Rh_2(OAc)_3(bpy)(MeOH)(H_2O)_2](OAc){\cdot}H_2O$. Anal. Calcd for $C_{19}H_{30}N_2O_{12}Rh_2$: C, 33.35; H, 4.42; N, 4.09. Found: C,

(7) Rubin, J. R. *Acta Crystallogr.* **1991**, *C47*, 1714.
(8) (a) Sherman, S. E.; Gibson, D.; Wang, A. H. J.; Lippard, S. J. *Science* **1985**, *230*, 412. (b) Sherman, S. E.; Gibson, D.; Wang, A. H. J.; Lippard, S. J. *J. Am. Chem. Soc.* **1988**, *110*, 7368.
(9) Admiraal, G.; van der Veer, J. L.; de Graaf, R. A. G.; den Hartog, J. H. J.; Reedijk, J. *J. Am. Chem. Soc.* **1987**, *110*, 7368.
(10) (a) Rosenberg, B. *Cancer* **1985**, *55*, 2303. (b) *Platinum Coordination Complexes in Chemotherapy*; Hacker, M. P., Douple, E. B., Krakoff, I. H., Eds.; Nijhoff Publishers: Boston, MA, 1984. (c) Platinum, Gold, and other Metal Chemotherapeutic Agents. *ACS Symp. Ser.* **1983**, *No.* 209. (d) Einhorn, L. H. *Cancer Res.* **1981**, *41*, 3275.
(11) (a) Köpf, H.; Kopf-Maier, P. *Angew. Chem., Int. Ed. Engl.* **1979**, *18*, 477. (b) Kopf-Maier, P.; Köpf, H. *Z. Naturforsch, B.: Anor. Chem., Org. Chem.* **1979**, *343*, 805.
(12) Köpf, H.; Kopf-Maier, P. *Platinum, Gold and Other Metal Chemotherapeutic Agents*; Lippard, S. J., Ed.; ACS Symposium Series: American Chemical Society: Washington, DC, 1983; Vol. 209, p 315.
(13) (a) McLaughlin, M. L.; Cronan, J. M., Jr.; Schaller, T. R.; Snelling, R. D. *J. Am. Chem. Soc.* **1990**, *112*, 8949. (b) Toney, J. H.; Brock, C. P.; Marks, T. J. *J. Am. Chem. Soc.* **1986**, *108*, 7263.
(14) (a) Kuo, L. Y.; Sabat, M.; Tipton, A. L.; Marks, T. J. Presented at the Third Chemical Congress of North America, Toronto, June 1988; Abstract 410. (b) Kuo, L. Y.; Kanatzidis, M. G.; Marks, T. J. *J. Am. Chem. Soc.* **1987**, *109*, 7207. (c) Kuo, L. Y.; Kanatzidis, M. G.; Sabat, M.; Tipton, A. L.; Marks, T. J. *J. Am. Chem. Soc.* **1991**, *113*, 4027.
(15) (a) Lippard, S. J. *Science* **1982**, *218*, 1075. (b) van der Veer, J. L.; Ligtvoet, G. J.; van den Elst, H.; Reedjik, J. *J. Am. Chem. Soc.* **1986**, *108*, 3860.
(16) Halpern, J.; Kimura, E.; Molin-Case, J.; Wong, C. S. *J. Chem. Soc., Chem. Commun.* **1971**, 1207.
(17) Pasternak, H.; Pruchnik, F. *Inorg. Nucl. Chem. Lett.* **1976**, *12*, 591.
(18) Pruchnik, F.; James, B. R.; Kvintovics, P. *Can. J. Chem.* **1986**, *64*, 936.
(19) (a) Collin, J. P.; Jouaiti, A.; Sauvage, J. P.; Kaska, W. C.; McLoughlin, M. A.; Keder, N. L.; Harrison, W. T. A.; Stucky, G. D. *Inorg. Chem.* **1990**, *29*, 2238. (b) Baker, A. T.; Tikkanen, W. R.; Kaska, W. C.; Ford, P. C. *Inorg. Chem.* **1984**, *23*, 3254. (c) Thummel, R. P.; Lefoulon, F.; Williamson, D.; Chavan, M. *Inorg. Chem.* **1986**, *25*, 1675. (d) Tikkanen, W. R.; Binamira-Soriaga, E.; Kaska, W. C.; Ford, P. C. *Inorg. Chem.* **1983**, *22*, 1147. (e) Tikkanen, W. R.; Binamira-Soriaga, E.; Kaska, W. C.; Ford, P. C. *Inorg. Chem.* **1984**, *23*, 141.
(20) Perlepes, S. P.; Huffman, J. C.; Matonic, J. H.; Dunbar, K. R.; Christou, G. *J. Am. Chem. Soc.* **1991**, *113*, 2770.
(21) Rempel, G. A.; Legzdins, P.; Smith, H.; Wilkinson, G. *Inorg. Synth.* **1972**, *13*, 90.
(22) (a) Telser, J.; Drago, R. S. *Inorg. Chem.* **1984**, *23*, 1798. (b) Baranovskii, I. B.; Golubnichaya, M. A.; Dikareva, L. M.; Shchelokov, R. N. *Russ. J. Inorg. Chem.* (*Engl. Transl.*) **1984**, *29*, 872. (c) Baranovskii, I. B.; Golubnichaya, M. A.; Zhilyaev, A. N.; Shchelokov, R. N. *Soviet J. Coord. Chem.* (*Engl. Transl.*) **1988**, 369. (d) Pimblett, G.; Garner, C. D.; Clegg, W. *J. Chem. Soc., Dalton Trans.* **1986**, 1257.

Pictiva EX2017
Samsung v Pictiva
IPR2024-01094

Table I. Crystallographic Data for Complexes **3**, **5**, and **7**

param	3	5	7
formula	$C_{18}H_{20}N_2O_8Rh_2$	$C_{26}H_{26}F_{12}N_2O_{10}Rh_2$	$C_{24}H_{29}B_2F_8N_7O_4Rh_2$
M_r	598.18	970.04	858.96
cryst system	triclinic	monoclinic	triclinic
space group	$P\bar{1}$	Pc	$P\bar{1}$
temp, °C	−172	−105	−170
a, Å	9.883(3)	10.683(8)	12.381(2)
b, Å	13.078(5)	9.170(8)	14.301(2)
c, Å	8.323(2)	17.783(1)	12.246(2)
α, deg	97.02(2)	90.00	94.60(1)
β, deg	106.90(1)	103.52(7)	105.84(1)
γ, deg	94.29(2)	90.00	117.42(1)
V, Å^3	1015	1693	1797
ρ_{calc}, g cm^{-3}	1.958	1.862	1.588
Z	2	2	2
cryst dimens, mm	0.25 × 0.25 × 0.25	0.27 × 0.09 × 0.99	0.14 × 0.24 × 0.40
radiation, Å	0.710 69	0.710 69	0.710 69
abs coeff, cm^{-1}	16.485	10.774	9.810
data collcd	$6° < 2\theta < 45°$	$4° < 2\theta < 50°$	$6° < 2\theta < 45°$
unique data	2636	2493	4723
averaging R	0.043	0.045	0.014
obsd data	1959, $F > 2.33\sigma(F)$	2493, $F > 3\sigma(F)$	4201, $F > 3\sigma(F)$
R, %[a]	4.72	5.10	4.92
R_w, %[b]	4.50	5.80	5.74

[a] $R = \sum||F_o| - |F_c||\sum|F_o|$. [b] $R_w = [\sum w(|F_o| - |F_c|)^2/\sum w|F_o|^2]^{1/2}$, where $w = 1/\sigma^2(|F_o|)$.

33.73; H, 4.09; N, 4.31. ^{1}H NMR in CD_3OD (ppm): O_2CCH_3, 2.309 (s, 3), 2.250 (s, 3), 1.876 (s, 3), 1.302 (s, 3); CH_3OH(eq), 3.339 (s, 3); CH_3OH(ax; free CH_3OH), 3.300 (s), bpy, 8.464 (d, 1), 8.431 (d, 1), 8.345 (d, 1), 8.339 (d, 1), 8.137 (td, 1); 8.136 (td, 1), 7.641 (m, 1), 7.635 (m, 1). ^{13}C{^{1}H} NMR of the bpy region (ppm): 123.8, 124.0, 127.5, 127.6, 139.6, 139.7, 152.2, 152.8, 158.8, 159.1. IR data (KBr pellet, cm^{-1}): 3438 (s, br), 3119 (m), 3081 (m), 2980 (m), 2930 (m), 1554 (s), 1545 (s), 1434 (s), 1409 (s), 766 (m), 727 (m), 708 (m). Electronic spectrum in MeOH [λ (ε)]: 226 (13 665), 254 (15 788), 294 (14 375), 424 (2010), 598 (206). The conductivity in MeOH is 56.13 S cm^2 mol^{-1} based on a molecular weight of 695 g/mol. FAB mass spectrum (*p*-nitrobenzyl alcohol as matrix) gives a peak at m/z 539 corresponding to the $[Rh_2(OAc)_3(bpy)]^+$ fragment.

$Rh_2(O_2CCF_3)_4(bpy)(THF)(H_2O)\cdot THF$ (5). A suspension of **2** (100 mg, 0.130 mmol) in CH_2Cl_2 (10 mL) was treated with a solution of bpy (20 mg, 0.13 mmol) in CH_2Cl_2 (5 mL) under anaerobic conditions. An immediate color change from blue to green was noted, and a green precipitate began to form. When precipitation was complete, the solid was collected by filtration and washed with CH_2Cl_2. The solid was redissolved in minimal THF, and hexanes were allowed to slowly diffuse into the resulting solution. Well-formed, green X-ray-quality crystals of **5** formed within 2 days; these were collected by filtration and washed with CH_2Cl_2. The yield was 0.068 g, 58%.

$Rh_2(O_2CCF_3)_4(bpy)(H_2O)_2$ (5′). A solution of **2** (40 mg, 51 μmol) in millipore grade H_2O (10 mL) was treated with solid bpy (8 mg, 51 μmol) followed by gentle heating for 15 min. The resulting green precipitate was collected by filtration and dried *in vacuo*. The solid was washed with hexanes to remove excess bpy and dried again *in vacuo*. The yield was essentially quantitative. ^{1}H NMR in $(CD_3)_2CO$ (ppm): 4.65 (s, 2), 7.69 (t, 1), 8.24 (t, 1), 8.35 (d, 1), 8.50 (d, 1). ^{19}F NMR ($CFCl_3$) in $(CD_3)_2CO$ (ppm): −76.48 (s, 1), −76.69 (s, 1). IR data (KBr pellet, cm^{-1}): 1690 (s), 1640 (s), 1470 (m), 1450 (m), 1430 (m), 1200 (s), 1150 (s), 870 (m), 790 (m), 760 (m), 740 (m), 730 (m). Electronic spectrum in Me_2CO [λ (ε)]: 610 (290), 379 (2794).

$[Rh_2(OAc)_2(bpy)(MeCN)_4](BF_4)_2\cdot MeCN$ (7). Under a nitrogen atmosphere, a stirring solution of **6** (200 mg, 0.276 mmol) in freshly distilled MeCN (10 mL) was treated with solid bpy (43 mg, 0.28 mmol). An immediate color change from violet to a deep red was noticed. After 24 h, the resulting solution was filtered and layered with Et_2O (15 mL). Red platelike crystals of X-ray quality appeared within 3 days. The crystals were collected by filtration and washed with Et_2O (5 mL). The yield was 0.157 g, 68%. Anal. Calcd for $C_{24}H_{29}B_2F_8N_7O_4Rh_2$: C, 33.56; H, 3.40; N, 11.41. Found: C, 33.41; H, 3.46; N, 11.32. ^{1}H NMR in CD_3CN (ppm): O_2CCH_3, 1.887 (s, 6); MeCN(eq), 2.243 (s, 6); MeCN(ax; free MeCN), 1.954 (s, 6); bpy, 8.587 (d, 2), 8.431 (d, 2), 8.233 (td, 2), 7.758 (td, 2). IR data (Nujol mull, cm^{-1}): 2332 (w), 2309 (w), 2280 (w), 2249 (w), 1564 (s), 1455 (s), 1061 (s), 777 (m), 729 (m), 713 (m). Electronic spectrum in MeCN [λ (ε)]: 364 (2245), 544 (1144), 690 (120).

X-ray Crystallography. Data were collected on $Rh_2(OAc)_4(bpy)$ (**3**) and $[Rh_2(OAc)_2(bpy)(MeCN)_4](BF_4)_2\cdot MeCN$ (**7**) using a Picker four-circle diffractometer; details of the diffractometry, low-temperature facilities, and computational procedures employed by the Molecular Structure Center are available elsewhere.[23] Data on $Rh_2(O_2CCF_3)_4(bpy)(THF)(H_2O)$ (**5**) were collected on a Nicolet P3/F updated to a Siemens P3/V diffractometer. General procedures are described elsewhere,[24] and the structure solution and refinement were carried out using the software package TEXSAN.[25] A rotational photograph was used to locate 13 reflections from which a preliminary cell was indexed. An accurate cell was determined from 25 reflections ranging in 2θ from 15 to 25°. Three or four standard reflections measured periodically throughout data collection revealed negligible decay for all three complexes.

On the basis of the Laue symmetry, the data indicated space groups $P\bar{1}$ or $P1$ (**3** and **7**) and Pc or $P2/c$ (**5**); $P\bar{1}$ in the former cases and Pc in the latter case were confirmed by subsequent successful structural solution and refinement. Heavy atoms were located by direct methods (MULTAN or MITHRIL),[26] and all other atoms, by difference Fourier maps. An absorption correction was performed on **5** after all non-hydrogen atoms had been refined isotropically, using the program DIFABS.[27] All refinements were by full-matrix least-squares. For complex **3**, all non-hydrogen atoms were well-behaved and all hydrogen atoms were clearly visible in a difference Fourier synthesis phased on the non-hydrogen parameters. The non-hydrogen atoms were refined anisotropically and the hydrogen atoms isotropically in the final cycles. For complex **5**, all atoms were readily located. The hydrogen atoms were included in fixed, calculated positions for the final refinement cycles; all non-hydrogen atoms were refined anisotropically except for the interstitial THF molecule. For complex **7**, all non-hydrogen atoms of the cation were well-behaved but positional disorder was encountered for the anions and interstitial MeCN molecules. The anions were modeled with three BF_4^- units, one with 100% occupancy and the others with 50% occupancy each. The MeCN electron density was modeled as two 50%-occupancy molecules; one of the latter and one anion position are mutually exclusive in that they are within bonding distance. All non-hydrogen atoms were refined anisotropically, except those of the disordered MeCN molecule. Hydrogen atoms were included in the final cycles in fixed calculated positions, except those for the disordered MeCN, which were omitted. Final values of discrepancy indices R and R_w are included in Table I.

(23) Chisholm, M. H.; Folting, K.; Huffman, J. C.; Kirkpatrick, C. C. *Inorg. Chem.* **1984**, *23*, 1021.
(24) (a) Cotton, F. A.; Frenz, B. A.; Deganello, G.; Shaver, A. *J. Organomet. Chem.* **1973**, 227. (b) Bino, A.; Cotton, F. A.; Fanwick, P. E. *Inorg. Chem.* **1979**, *18*, 3558.
(25) TEXSAN-TEXRAY Structure Analysis package, Molecular Structure Corp., 1985.
(26) Gilmore, G. J. *J. Appl. Crystallogr.* **1984**, *17*, 42.
(27) Walker, N.; Stuart, D. *Acta Crystallogr.* **1983**, *A39*, 158.

Pictiva EX2017
Samsung v Pictiva
IPR2024-01094

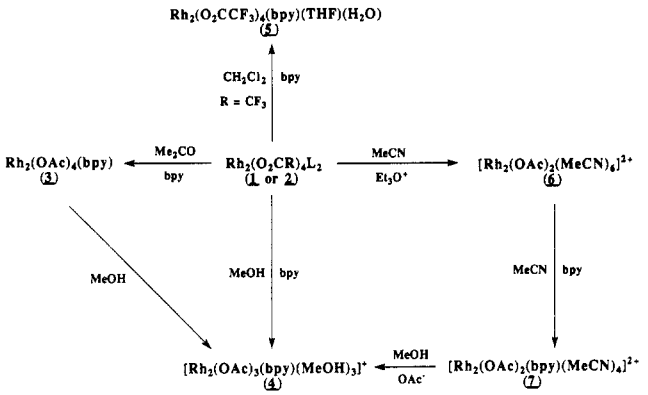

Figure 1. Schematic representation of the transformations mentioned in the text, together with the compound numbering scheme.

Other Measurements. Infrared (KBr pellet or Nujol mull) and electronic spectra were recorded on Nicolet 510P or Perkin-Elmer 599 and Hewlett-Packard 8452A or Hitachi U2000 spectrophotometers, respectively. ^{1}H NMR were recorded on Varian XL-300 or Bruker AM-500 spectrometers. Chemical shifts are quoted on the δ scale (shifts downfield are positive) and referenced *versus* solvent. Conductivity studies were performed on a YSI Model 31A conductance bridge; no compensation for solvent was incorporated. Elemental microanalyses were performed by Atlantic Microlab, Inc.

Results

Syntheses. For convenience, the various transformations described in the text are summarized schematically in Figure 1, which is also a convenient reminder of the compound numbering scheme.

The initial reaction explored was that between $Rh_2(OAc)_4(MeOH)_2$ (**1**) and 1 equiv of bpy in either MeCN or Me_2CO. Both solvents facilitate a rapid reaction, a color change to deep green, and the subsequent precipitation of green $Rh_2(OAc)_4(bpy)$ (**3**), whose identity was established by crystallography. MeCN was the solvent originally employed, but it leads to a slightly contaminated product in only modest yield (*ca.* 40%). Acetone was subsequently found to be far superior from both a purity and yield (95%) viewpoint, and it is now the solvent routinely employed. The reaction is summarized in eq 1. Complex **3** is

$$\underset{\mathbf{1}}{Rh_2(OAc)_4(MeOH)_2} + bpy \rightarrow \underset{\mathbf{3}}{Rh_2(OAc)_4(bpy)} + 2MeOH \quad (1)$$

air-stable but only sparingly soluble in most common solvents. It is moderately soluble in CH_2Cl_2 and $CHCl_3$, which allows for solution characterization (but resonances in the ^{1}H NMR spectra due to decomposition products were observed even in freshly-prepared solutions). Significant decomposition occurs within 1–2 h, and faster if the solvents are not freshly distilled. NMR spectra and visual changes indicate *rapid* decomposition in H_2O, MeCN, and DMSO. Complex **3** appears to be insoluble in MeOH but does slowly dissolve on prolonged stirring to give an emerald-green solution; this, however, does not contain complex **3** but instead $[Rh_2(OAc)_3(bpy)(MeOH)_3](OAc)$ (**4**). The latter can be readily isolated by addition of Et_2O, and its identity has been established by a number of methods (*vide infra*). The MeOH-induced transformation of **3** to **4** is summarized in eq 2.

$$\underset{\mathbf{3}}{Rh_2(OAc)_4(bpy)} \xrightarrow{MeOH} \underset{\mathbf{4}}{[Rh_2(OAc)_3(bpy)(MeOH)_3](OAc)} \quad (2)$$

With products **3** and **4** identified, a parallel reaction employing the more labile starting material $Rh_2(O_2CCF_3)_4(Me_2CO)_2$ (**2**) was investigated. Due to solubility considerations, the reaction was performed in CH_2Cl_2 and the product recrystallized from THF/hexanes; this procedure gave green $Rh_2(O_2CCF_3)_4(bpy)$-(THF)(H_2O) (**5**) in a form suitable for structural characterization. Its formation is summarized in eq 3. An improved procedure for

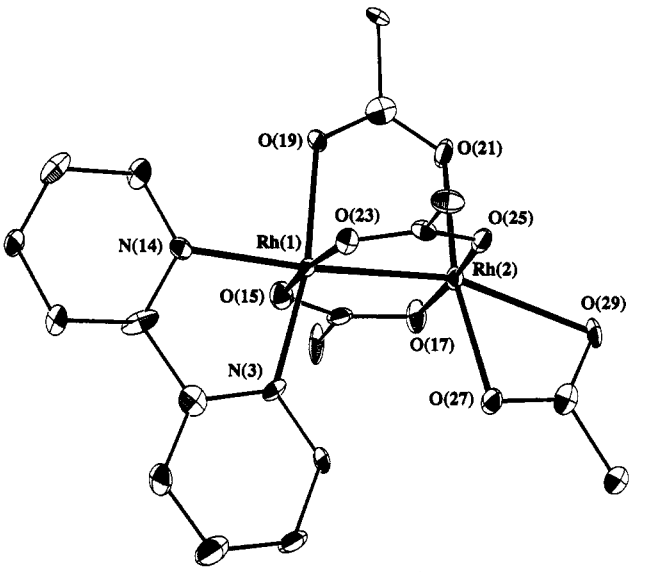

Figure 2. ORTEP representation of complex **3** at the 50% probability level. Carbon atoms are numbered sequentially clockwise from N(3) to N(14). Other carbon atoms are numbered sequentially from labeled atoms.

$$\underset{\mathbf{2}}{Rh_2(O_2CCF_3)_4(Me_2CO)_2} + bpy \xrightarrow[THF/H_2O]{CH_2Cl_2} \underset{\mathbf{5}}{Rh_2(O_2CCF_3)_4(bpy)(THF)(H_2O)} \quad (3)$$

the essentially quantitative synthesis of the diaquo version, $Rh_2(O_2CCF_3)_4(bpy)_2(H_2O)_2$ (**5′**), makes use of H_2O as the reaction solvent. The product is insoluble in H_2O, allowing for its convenient isolation. The same product is also obtained from an Me_2CO reaction medium, as confirmed by spectroscopic comparisons.

Mono-bpy complexes may also be prepared using $[Rh_2(OAc)_2(MeCN)_6](BF_4)_2$ (**6**), in which two of the bridging AcO^- groups in **1** have been previously removed with Et_3O^+ in MeCN. Treatment of **6** with bpy readily leads to deep-red $[Rh_2(OAc)_2(bpy)(MeCN)_4](BF_4)_2$ (**7**), the bpy group displacing two equatorial MeCN molecules (eq 4) as confirmed crystallographically. Treatment of **7** with NaOAc in MeOH slowly gives a color change to green; as expected, the NMR spectrum indicates the product to be complex **4**. The transformation is summarized in eq 5.

$$\underset{\mathbf{6}}{[Rh_2(OAc)_2(MeCN)_6]^{2+}} + bpy \rightarrow \underset{\mathbf{7}}{[Rh_2(OAc)_2(bpy)(MeCN)_4]^{2+}} + 2MeCN \quad (4)$$

$$\underset{\mathbf{7}}{[Rh_2(OAc)_2(bpy)(MeCN)_4]^{2+}} + AcO^- \xrightarrow{MeOH} \underset{\mathbf{4}}{[Rh_2(OAc)_3(bpy)(MeOH)_3]^+} + 4MeCN \quad (5)$$

Description of Structures. ORTEP plots of complexes **3** and **5** and the cation of complex **7** are presented in Figures 2–4, respectively; selected metric parameters are presented in Tables II–VII. Complex **3** crystallizes in the triclinic space group $P\bar{1}$ with no crystallographically-imposed symmetry but with idealized C_s symmetry (mirror plane: N(3), N(14), Rh(1), Rh(2), O(27), O(29)). Two Rh^{II} centers are bridged by three AcO^- groups in the familiar $\eta^1:\eta^1:\mu_2$ mode across a Rh–Rh single-bond distance

Pictiva EX2017
Samsung v Pictiva
IPR2024-01094

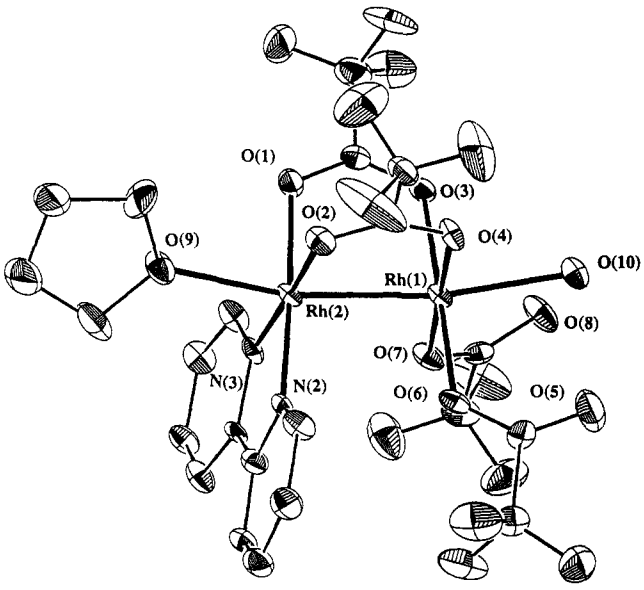

Figure 3. ORTEP representation of complex **5** at the 50% probability level. Carbon atoms C(8)–C(17) and C(19)–C(22) belong to bpy and THF rings; respectively. The other carbons are carboxylate atoms.

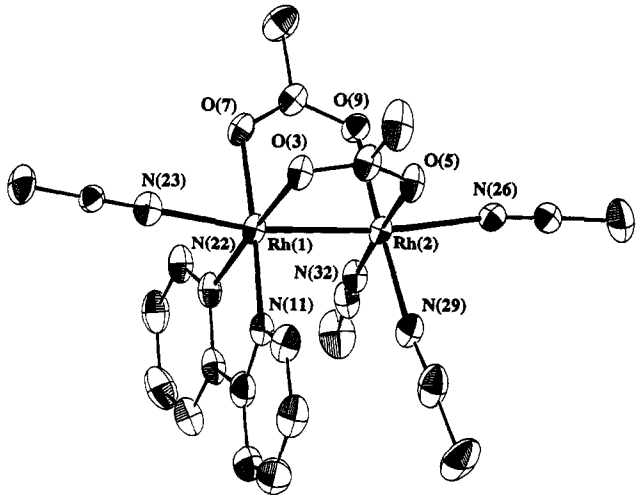

Figure 4. ORTEP representation of $[Rh_2(OAc)_2(bpy)(MeCN)_4]^{2+}$, the cation of complex **7**, at the 50% probability level. Carbon atoms are numbered sequentially clockwise from N(11) to N(22). Other carbon atoms are numbered sequentially from labeled atoms.

of 2.475(2) Å.[28] Octahedral coordination at Rh(1) and Rh(2) is completed by a chelating bpy and a chelating AcO^-, respectively. The bpy nitrogen atoms occupy one axial and one equatorial site (*ax-eq*) with the expected slight difference in Rh–N bond lengths (2.120(10) *vs* 2.039(9) Å, respectively). Much greater asymmetry is observed in the chelating AcO^- group at Rh(2), which is an extremely rare example of an asymmetrically-chelating carboxylate, symmetric chelation being much more common.[29] The axial/equatorial disposition of the two oxygen atoms leads to large differences in Rh–O distances (Rh(2)–O(29) = 2.466(8) Å; Rh(2)–O(27) = 2.051(8) Å). In addition, the small acetate bite angle (57.1(3)°) prevents O(29) from lying on the true axial position (Rh(1)–Rh(2)–O(29) = 163.51 (19)°).

Numerous attempts to obtain crystals of complex **4** in a form suitable for crystallographic characterization have all proven

Table II. Selected Fractional Coordinates (×10⁴) and Isotropic Thermal Parameters (×10, Å²) for Complex **3**

atom	x	y	z	B_{eq}[a]
Rh(1)	9315(1)	2067(1)	1979(1)	8
Rh(2)	7307(1)	2691(2)	−70(1)	9
N(3)	10643(10)	3377(7)	3207(12)	9
C(4)	10462(13)	4358(10)	2987(17)	21
C(5)	11450(15)	5194(10)	3863(18)	25
C(6)	12655(15)	5025(10)	5117(18)	27
C(7)	12884(14)	4025(10)	5366(17)	21
C(8)	11882(12)	3216(9)	4388(15)	15
C(9)	12074(14)	2120(9)	4625(5)	17
C(10)	13235(13)	1809(9)	5812(14)	12
C(11)	13284(13)	767(9)	5922(17)	18
C(12)	12184(15)	35(10)	4852(17)	20
C(13)	11040(13)	392(10)	3710(5)	14
N(14)	10980(10)	1405(7)	3605(12)	10
O(15)	10300(8)	2007(6)	121(10)	14
C(16)	9740(13)	2371(9)	−1227(15)	14
O(17)	8542(8)	2714(6)	−1649(10)	15
C(18)	10566(13)	2403(11)	−2431(17)	19
O(19)	8277(8)	621(6)	1023(10)	13
C(20)	7202(13)	465(9)	−260(15)	14
O(21)	6632(8)	1165(6)	−972(10)	15
C(22)	6596(13)	−656(10)	−933(17)	17
O(23)	8139(8)	2194(6)	3646(9)	11
C(24)	6862(12)	2408(9)	3127(14)	11
O(25)	6240(8)	2640(6)	1690(9)	11
C(26)	6008(15)	2367(11)	4372(18)	17
O(27)	7608(8)	4281(6)	424(10)	16
C(28)	6576(13)	4489(9)	−790(15)	14
O(29)	5749(8)	3790(6)	−1814(10)	16
C(30)	6418(15)	5615(10)	−906(19)	21

[a] Equivalent isotropic values for atoms refined anisotropically.

unsuccessful, but its identity was deduced by other means: (i) Elemental analysis indicates retention of the 4:1:2 = AcO:bpy: Rh ratio of **3**. (ii) FAB mass spectrometry gives the highest observed m/z peak at 539 corresponding to $[Rh_2(OAc)_3(bpy)]^+$. (iii) A conductivity measurement in MeOH gives a value of 56 S cm² mol⁻¹, consistent with a 1:1 electrolyte. (iv) NMR data in CD_3OD show four AcO^- and eight bpy resonances (*vide infra*) indicating low symmetry. (v) Attainment of **4** by treatment of **7** with NaOAc in MeOH indicates possible structural similarity to crystallographically-characterized **7**. On the basis of the combined observations above, complex **4** is formulated as $[Rh_2(OAc)_3(bpy)(MeOH)_3](OAc)$ with the structure of C_1 symmetry shown as follows:

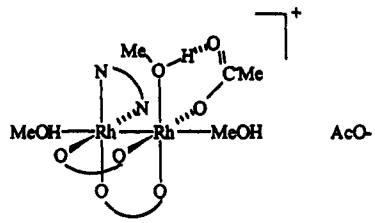

4

The complex is thus proposed to possess an *eq-eq* bpy group, together with one terminal AcO^- and one MeOH in the other two equatorial sites. We have no evidence for a hydrogen bond between the latter in the solid state, but this seems reasonable given their proximity (alternatively, the AcO^- could be hydrogen-bonded to the axial MeOH group.). Additional evidence for the proposed structure of **4** will be discussed in the following paragraphs.

The structure of complex **5** contains an *eq-eq* bpy at Rh(2) and two terminal $CF_3CO_2^-$ groups at Rh(1) to complement the two bridging $CF_3CO_2^-$ groups. The Rh(1)–Rh(2) distance (2.520(3) Å) is slightly greater than in **3**, which is not unusual since all $CF_3CO_2^-$ complexes of dirhodium show this trend compared to the AcO^- complexes, and in addition complex **5** has fewer bridging groups than **3**. The structure of **5** provides support for the proposed

(28) (a) Felthouse, T. R. *Prog. Inorg. Chem.* **1982**, *29*, 73. (b) Cotton, F. A.; Walton, R. A. Multiple Bonds Between Metal Atoms; Wiley: New York, 1982; Chapter 7. (c) Constable, E. C. *Coord. Chem. Rev.* **1986**, *73*, 59.

(29) (a) Hursthouse, M. B.; Malik, K. M. A. *J. Chem. Soc., Dalton Trans.* **1979**, 409. (b) Roberts, P. J.; Ferguson, G.; Goel, R. G.; Ogini, W. O.; Resitvo, R. J. *J. Chem. Soc., Dalton Trans.* **1978**, 253. (c) Alcock, N. W.; Tracy, V. L. *Acta Crystallogr., Sect. B* **1979**, *B35*, 80. (d) Mehrotra, R. C.; Bohra, R. *Metal Carboxylates*; Academic Press: London, 1983.

Pictiva EX2017
Samsung v Pictiva
IPR2024-01094

Table III. Selected Fractional Coordinates and Isotropic Thermal Parameters (Å^2) for Complex **5**

atom	x	y	z	B_{iso}
Rh(1)	0.4354	0.2472(1)	0.2212	2.08(4)
Rh(2)	0.5976(1)	0.2145(1)	0.34804(8)	2.09(4)
F(1)	0.132(1)	−0.047(1)	0.3098(9)	6.7(6)
F(2)	0.096(2)	0.173(1)	0.3318(8)	6.9(7)
F(3)	−0.027(1)	0.070(2)	0.2405(8)	7.2(7)
F(4)	0.567(2)	−0.197(2)	0.1412(7)	8.8(7)
F(5)	0.616(2)	−0.267(1)	0.258(1)	11(1)
F(6)	0.745(1)	−0.159(2)	0.214(1)	9(1)
F(7)	0.327(1)	0.690(1)	0.3140(7)	6.7(6)
F(8)	0.293(2)	0.793(1)	0.2036(8)	7.9(7)
F(9)	0.153(1)	0.661(1)	0.2351(9)	7.1(7)
F(10)	0.812(1)	0.306(2)	0.1309(8)	7.3(7)
F(11)	0.755(1)	0.519(1)	0.1448(8)	6.6(6)
F(12)	0.904(1)	0.420(2)	0.2295(7)	7.6(7)
O(1)	0.730(1)	0.295(1)	0.2905(6)	3.0(4)
O(2)	0.629(1)	0.010(1)	0.3055(7)	3.2(5)
O(3)	0.580(1)	0.340(1)	0.1816(6)	2.6(4)
O(4)	0.496(1)	0.050(1)	0.1909(6)	2.8(4)
O(5)	0.138(2)	0.136(2)	0.1548(8)	6.0(7)
O(6)	0.294(1)	0.155(1)	0.2634(6)	2.8(5)
O(7)	0.376(1)	0.443(1)	0.2516(6)	3.1(5)
O(8)	0.305(1)	0.538(1)	0.1333(6)	4.4(6)
O(9)	0.769(1)	0.167(1)	0.4453(7)	4.4(5)
O(10)	0.317(1)	0.255(1)	0.0975(6)	2.9(4)
N(2)	0.475(1)	0.145(1)	0.4100(7)	2.6(5)
N(3)	0.572(1)	0.399(1)	0.3977(6)	2.4(5)
C(1)	0.183(1)	0.129(2)	0.224(1)	2.7(6)
C(2)	0.094(2)	0.079(2)	0.274(1)	3.6(7)
C(3)	0.326(1)	0.539(2)	0.204(1)	2.7(6)
C(4)	0.275(2)	0.673(2)	0.241(1)	3.8(8)
C(5)	0.576(2)	−0.018(2)	0.239(1)	2.9(7)
C(6)	0.623(2)	−0.160(2)	0.210(1)	3.5(7)
C(7)	0.689(2)	0.341(2)	0.222(1)	2.5(6)
C(8)	0.633(2)	0.529(2)	0.3913(9)	3.2(6)
C(9)	0.620(2)	0.650(2)	0.435(1)	3.7(7)
C(10)	0.539(2)	0.640(2)	0.4863(9)	3.0(6)
C(11)	0.479(2)	0.507(2)	0.4958(9)	3.4(7)
C(12)	0.493(1)	0.391(2)	0.4499(8)	2.3(5)
C(13)	0.439(1)	0.248(1)	0.4544(8)	2.6(5)
C(14)	0.359(1)	0.214(2)	0.5023(8)	3.0(6)
C(15)	0.317(2)	0.067(2)	0.506(1)	3.6(7)
C(16)	0.434(2)	0.008(1)	0.4106(9)	3.1(6)
C(17)	0.356(2)	−0.035(2)	0.459(1)	4.1(8)
C(18)	0.791(2)	0.399(2)	0.182(1)	4.4(9)
C(19)	0.776(3)	0.169(3)	0.526(1)	8(1)
C(20)	0.871(2)	0.069(3)	0.433(2)	7(1)
C(21)	0.966(2)	0.064(4)	0.508(1)	8(1)
C(22)	0.905(3)	0.126(5)	0.566(1)	12(2)

structure of **4**, in that they share the common features of an *eq-eq* bpy and terminal equatorial carboxylates. An interesting structural feature of **5** is the asymmetry in axial donor groups, *viz.*, THF at Rh(2) and H_2O at Rh(1). The latter is undoubtedly preferred due to the hydrogen-bonding interactions that it undergoes with the free carboxyl oxygen atoms O(5) and O(8) of the terminal $CF_3CO_2^-$ groups (O(5)··O(10) = 2.60(2) Å; O(8)··O(10) = 2.68(1) Å). With free rotation of the THF, complex **5** has idealized C_s symmetry.

The cation of complex **7** also possesses idealized C_s symmetry and a structure similar to that of **5** except that the terminal carboxylates and axial groups are all replaced by MeCN molecules. The Rh–Rh distance (2.540(1) Å) is slightly greater than that in **5**. As expected, bonds to axial MeCN groups (average 2.209 Å) are longer than to equatorial MeCN groups (average 1.984 Å).

Some comments pertinent to the structures of all three complexes, **3**, **5**, and **7**, are warranted. In each case, the presence of a single bpy group in a nonbridging ligation mode necessitates the formation of an asymmetric complex; the environments of the two Rh^{II} centers are thus distinctly different. In each case, there remain either two or three bridging carboxylates, which ensures retention of an essentially eclipsed conformation about the Rh–Rh bond, in contrast to, for example, $[Rh_2(MeCN)_{10}]^{4+}$, which has a staggered conformation.[30]

Table IV. Selected Fractional Coordinates (×10^4) and Isotropic Thermal Parameters (×10, Å^2) for Complex **7**

atom	x	y	z	B_{eq}[a]
Rh(1)	4531(1)	3007.8(4)	1993.6(5)	18
Rh(2)	3504.3(5)	989.6(4)	1901.7(5)	16
O(3)	5227(4)	2686(4)	755(4)	21
C(4)	5077(7)	1764(6)	448(7)	25
O(5)	4433(5)	937(4)	796(4)	24
C(6)	5691(9)	1614(7)	−401(9)	39
O(7)	2835(4)	2605(4)	683(4)	21
C(8)	1971(6)	1632(6)	230(6)	20
O(9)	2015(4)	819(4)	537(4)	22
C(10)	780(8)	1396(7)	−776(7)	33
N(11)	6143(5)	3439(5)	3346(5)	21
C(12)	7240(7)	3526(6)	3296(7)	27
C(13)	8300(8)	3787(7)	4278(8)	34
C(14)	8199(8)	3957(7)	5365(8)	35
C(15)	7089(8)	3894(6)	5459(7)	31
C(16)	6058(7)	3631(6)	4431(7)	28
C(17)	4823(7)	3569(5)	4385(6)	23
C(18)	4525(8)	3755(6)	5366(7)	33
C(19)	3326(8)	3694(7)	5207(8)	36
C(20)	2512(8)	3500(6)	4108(8)	31
C(21)	2880(7)	3341(6)	3153(7)	24
N(22)	3975(5)	3344(4)	3290(5)	21
N(23)	5293(6)	4669(5)	1769(5)	24
C(24)	5681(7)	5538(6)	1655(6)	20
C(25)	6181(8)	6629(6)	1504(7)	32
N(26)	2513(5)	−814(5)	1574(5)	19
C(27)	2049(7)	−1701(6)	1540(6)	21
C(28)	1455(9)	−2859(6)	1509(8)	38
N(29)	4932(6)	1081(5)	3229(5)	23
C(30)	5687(8)	1030(6)	3941(8)	36
C(31)	6653(9)	986(8)	4914(9)	50
N(32)	2544(5)	948(4)	2965(5)	19
C(33)	1921(8)	811(6)	3513(7)	29
C(34)	1156(9)	644(7)	4291(8)	39

[a] Equivalent isotropic values for atoms refined anisotropically.

Table V. Selected Bond Distances (Å) and Angles (deg) for Complex **3**

a. Bonds			
Rh(1)–Rh(2)	2.4754(15)	Rh(2)–O(17)	2.038(8)
Rh(1)–N(3)	2.039(9)	Rh(2)–O(21)	2.034(8)
Rh(1)–N(14)	2.120(10)	Rh(2)–O(25)	2.043(8)
Rh(1)–O(15)	2.050(8)	Rh(2)–O(27)	2.051(8)
Rh(1)–O(19)	2.033(7)	Rh(2)–O(29)	2.466(8)
Rh(1)–O(23)	2.053(7)		
b. Angles			
Rh(2)–Rh(1)–N(3)	104.69(26)	Rh(1)–Rh(2)–O(17)	87.22(22)
Rh(2)–Rh(1)–N(14)	175.07(26)	Rh(1)–Rh(2)–O(21)	85.61(22)
Rh(2)–Rh(1)–O(15)	86.64(22)	Rh(1)–Rh(2)–O(25)	87.27(21)
Rh(2)–Rh(1)–O(19)	86.03(22)	Rh(1)–Rh(2)–O(27)	106.86(21)
Rh(2)–Rh(1)–O(23)	86.70(22)	Rh(1)–Rh(2)–O(29)	163.51(19)
O(15)–Rh(1)–O(19)	91.2(3)	O(17)–Rh(2)–O(21)	90.2(3)
O(15)–Rh(1)–O(23)	173.3(3)	O(17)–Rh(2)–O(25)	174.4(3)
O(15)–Rh(1)–N(3)	88.9(3)	O(17)–Rh(2)–O(27)	90.1(3)
O(15)–Rh(1)–N(14)	91.9(3)	O(17)–Rh(2)–O(29)	88.8(3)
N(3)–Rh(1)–N(14)	80.0(4)	O(21)–Rh(2)–O(27)	167.5(3)
N(3)–Rh(1)–O(19)	169.3(3)	O(27)–Rh(2)–O(29)	57.1(3)

Solution Properties and ^{1}H NMR Data. The low solubility of complex **3** in solvents that do not transform it has hindered extensive investigation, but its adequate solubility in CH_2Cl_2 (and to a lesser extent $CHCl_3$) has permitted some solution studies to be performed. A conductivity measurement in CH_2Cl_2 indicated **3** to be a nonelectrolyte in solution, supporting the conclusion that the solid-state structure remains intact. More evidence for this was provided by the ^{1}H NMR spectrum of **3** in CD_2Cl_2 (Figures 5 and 6) that showed three methyl singlets at 2.18, 2.15, and 1.69 ppm in a 1:1:2 integration ratio and eight bpy resonances in the 7.4–9.7 ppm range (with some overlap in the *ca.* 8.3 ppm

(30) (a) Dunbar, K. R. *J. Am. Chem. Soc.* **1988**, *110*, 8247. (b) Dunbar, K. R.; Pence, L. E. *Inorg. Synth.* **1992**, *29*, 182.

Pictiva EX2017
Samsung v Pictiva
IPR2024-01094

Table VI. Selected Bond Distances (Å) and Angles (deg) for Complex **5**

a. Bonds			
Rh(1)–Rh(2)	2.520(3)	Rh(2)–O(1)	2.06(1)
Rh(1)–O(3)	2.03(1)	Rh(2)–O(2)	2.08(1)
Rh(1)–O(4)	2.03(1)	Rh(2)–O(9)	2.25(1)
Rh(1)–O(6)	2.02(1)	Rh(2)–N(2)	2.01(1)
Rh(1)–O(7)	2.02(1)	Rh(2)–N(3)	1.96(1)
Rh(1)–O(10)	2.27(1)		
b. Angles			
Rh(2)–Rh(1)–O(3)	86.6(3)	Rh(1)–Rh(2)–O(1)	85.5(3)
Rh(2)–Rh(1)–O(4)	86.4(3)	Rh(1)–Rh(2)–O(2)	85.2(3)
Rh(2)–Rh(1)–O(6)	92.0(3)	Rh(1)–Rh(2)–N(2)	97.3(3)
Rh(2)–Rh(1)–O(7)	93.5(3)	Rh(1)–Rh(2)–N(3)	99.2(3)
Rh(2)–Rh(1)–O(10)	169.3(3)	Rh(1)–Rh(2)–O(9)	167.8(3)
O(3)–Rh(1)–O(4)	88.2(4)	O(1)–Rh(2)–O(2)	87.5(4)
O(3)–Rh(1)–O(6)	178.5(5)	O(1)–Rh(2)–N(2)	176.1(4)
O(3)–Rh(1)–O(7)	91.8(4)	O(1)–Rh(2)–N(3)	95.7(5)
O(3)–Rh(1)–O(10)	87.1(4)	O(1)–Rh(2)–O(9)	85.5(5)
O(6)–Rh(1)–O(10)	94.4(4)	N(2)–Rh(2)–N(3)	81.2(5)
O(6)–Rh(1)–O(7)	87.7(4)	N(2)–Rh(2)–O(9)	92.1(5)

Table VII. Selected Bond Distances (Å) and Angles (deg) for Complex **7**

a. Bonds			
Rh(1)–Rh(2)	2.5395(8)	Rh(2)–O(5)	2.019(5)
Rh(1)–O(3)	2.054(4)	Rh(2)–O(9)	2.022(5)
Rh(1)–O(7)	2.053(5)	Rh(2)–N(26)	2.229(6)
Rh(1)–N(11)	2.001(6)	Rh(2)–N(29)	1.991(6)
Rh(1)–N(22)	2.001(6))	Rh(2)–N(32)	1.977(5)
Rh(1)–N(23)	2.188(6)		
b. Angles			
Rh(2)–Rh(1)–N(23)	170.89(16)	Rh(1)–Rh(2)–N(26)	172.69(14)
Rh(2)–Rh(1)–O(3)	85.35(13)	Rh(1)–Rh(2)–O(5)	85.99(13)
Rh(2)–Rh(1)–O(7)	85.74(13)	Rh(1)–Rh(2)–O(9)	85.73(13)
Rh(2)–Rh(1)–N(11)	95.26(16)	Rh(1)–Rh(2)–N(29)	96.97(17)
Rh(2)–Rh(1)–N(22)	94.76(16)	Rh(1)–Rh(2)–N(32)	97.30(16)
O(3)–Rh(1)–O(7)	89.29(9)	O(5)–Rh(2)–O(9)	89.52(20)
O(3)–Rh(10)–N(23)	88.37(20)	O(5)–Rh(2)–N(26)	89.51(19)
O(3)–Rh(1)–N(11)	94.55(21)	O(5)–Rh(2)–N(29)	90.27(22)
O(7)–Rh(1)–N(11)	176.10(20)	O(5)–Rh(2)–N(32)	176.69(20)
N(11)–Rh(1)–N(22)	81.24(33)	N(26)–Rh(2)–N(29)	88.79(22)
N(11)–Rh(1)–N(23)	91.80(22)	N(29)–Rh(2)–N(23)	89.72(24)

region). These are as expected from the C_s symmetry solid-state structure. Complex **3** precipitates from Me_2CO solution too rapidly to permit investigation of the solution species present; however, the corresponding propionate appears to be slightly more soluble and therefore precipitates more slowly. Thus, reaction of $Rh_2(O_2CEt)_4(MeOH)_2$ and 1 equiv of bpy in $(CD_3)_2CO$ gives a green solution that remains homogeneous during the recording of a ^1H NMR spectrum; the spectrum is as expected for a $Rh_2(O_2CEt)_4(bpy)$ molecule with the same structure as **3** (along with traces of unreacted starting material). Thus, we conclude that complex **3** is the only observable species in the preparative solution and that it possesses its C_s solid-state structure both in Me_2CO prior to precipitation and when redissolved in CH_2Cl_2.

In contrast to the solution behavior of **3** in Me_2CO and CH_2Cl_2, the dissolution of **3** in MeOH is accompanied by a structural change that yields **4**. The spectrum in CD_3OD (Figures 5 and 6) is distinctly different from that of **3** in CD_2Cl_2 and appeared to display four AcO^- peaks (1.30–2.31 ppm) and four bpy peaks, the latter suggesting the two halves of the bpy to be equivalent. It was difficult, however, to accept that a dinuclear structure could contain a bpy ligand bisected by a mirror plane and also possess four inequivalent AcO^- groups. We suspected that there were really eight separate bpy resonances occurring in unresolved pairs, and to ensure good resolution of overlapping multiplets, we resorted to 2D homonuclear *J*-resolved spectroscopy (Figure 7), which clearly indicates seven separate resonances, thereby confirming the inequivalence of the two bpy halves. In fact, although it is not obvious from the plot in Figure 7, the two resonances in the 8.2–8.4 ppm range were actually resolved in the 2D experiment; they possess almost identical chemical shifts (8.136 and 8.137 ppm) and are shown in Figure 7 where vertical "slices"

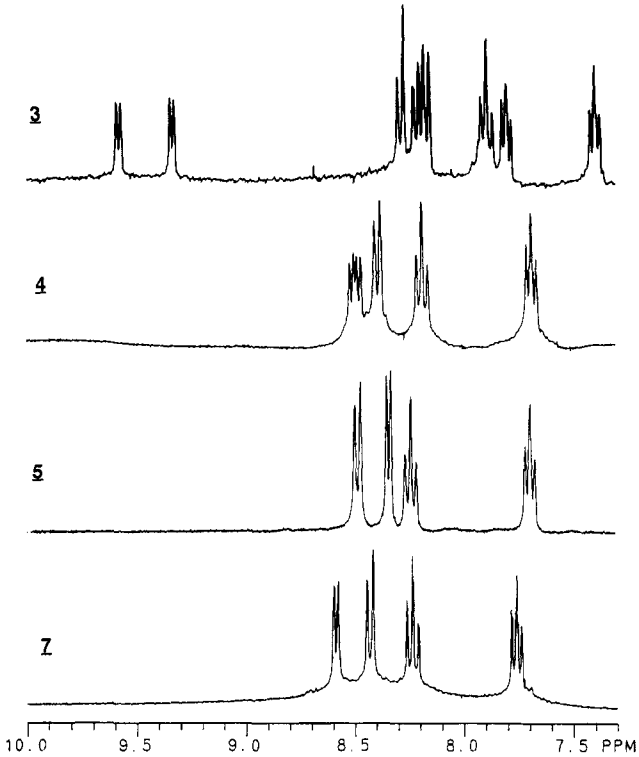

Figure 5. ^1H NMR spectra at 300 MHz in the aromatic region for complexes **3–5** and **7**.

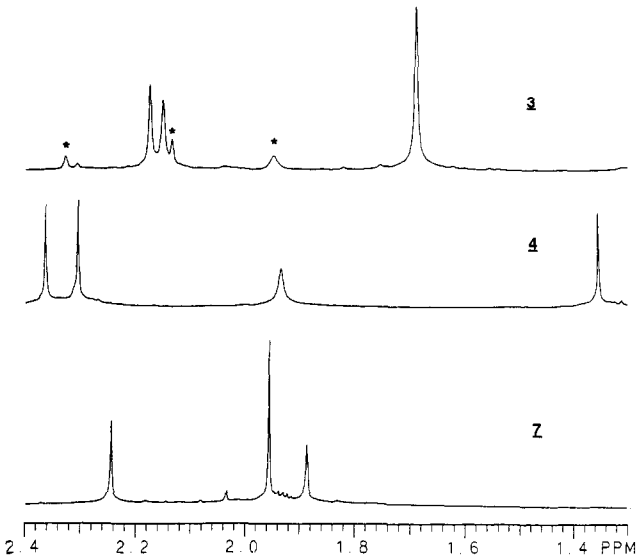

Figure 6. ^1H NMR spectra of 300 MHz in the acetate region for complexes **3**, **4**, and **7**. The peaks marked with an asterisk are due to decomposition products, and their intensities increase with time.

through the 2D matrix are shown. The presence of eight bpy proton resonces was further confirmed by selective homonuclear decoupling experiments; Figure 8 depicts the effects of selectively irradiating the four distinct bpy regions of the spectrum. It is clear that there are more than four multiplets; for example, the four features in the 8.4–8.5 ppm region simplify to two features only upon irradiation of the 7.6–7.7 ppm multiplet, supporting the conclusion that the 8.4–8.5 ppm features are two separate doublets rather than a doublet-of-doublets. These data support the structure of **4** depicted above in which the two halves of the bpy are in very similar but not identical environments. The free AcO^- was assigned to the 1.876 ppm resonance (Figure 6) on the basis of the increase in intensity of the latter upon addition of NaOAc and its disappearance upon addition of silver triflate, concomitant with precipitation of solid AgOAc. The presence of the equatorial MeOH was verified by recording the ^1H NMR spectrum immediately after dissolution of **4** in CD_3OD. A distinct

Pictiva EX2017
Samsung v Pictiva
IPR2024-01094

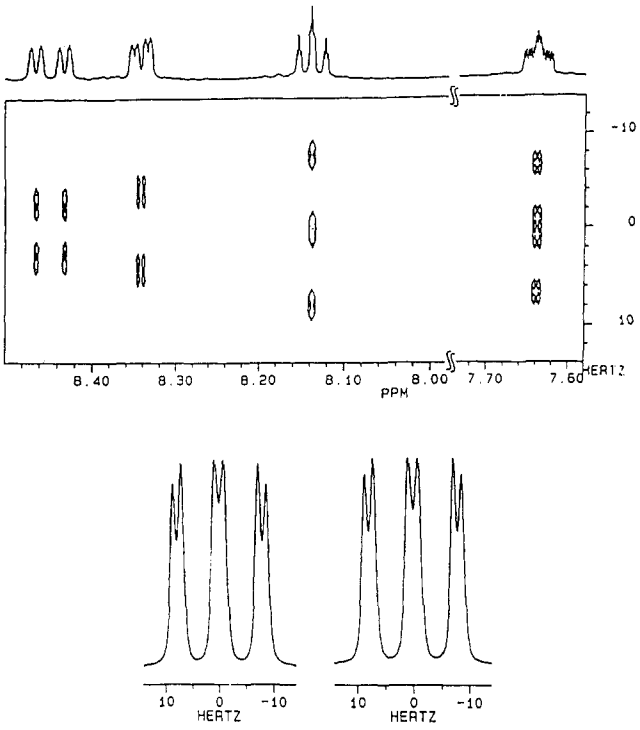

Figure 7. 2D homonuclear *J*-resolved NMR spectrum at 500 MHz in the aromatic region for complex **4**. The two multiplets in the bottom part of the figure are the two barely-resolved resonances in the *ca.* 8.14 ppm region.

resonance at 3.34 ppm was observed that disappeared after 10 min due to exchange with free CD_3OD (3.30 ppm). In contrast, exchange of *axially*-bound MeOH groups is much too rapid on the NMR time scale to give a distinct signal. Although it is soluble in MeCN, complex **4** gives a complicated spectrum in this solvent, suggesting that several species are interconverting in solution.

After recognizing that complex **3** converts to **4** in MeOH, we sought to monitor by ^1H NMR the reaction of $Rh_2(OAc)_4(MeOH)_2$ with ~1 equiv of bpy in CD_3OD. A slow reaction occurs that gives, in addition to free bpy resonances, features spanning the 6.7–9.2 ppm range. After 2 h, resonances in the 7.5–8.8 ppm range attributable to complex **4** and free bpy were present, along with remaining resonances spanning the 6.7–9.2 ppm range. The latter are reminiscent of the NMR spectrum for **3** (Figure 5) in that the resonances are spread out over a wide range of chemical shifts, which we take as an indication that an *ax-eq* bpy group is present, although overall the molecular arrangement is not identical to that of **3**.

The NMR spectra of complexes **5** and **7** each exhibit four bpy signals, consistent with C_s symmetry (Figure 5), and as expected, **7** exhibits only one AcO^- resonance (1.89 ppm). The spectrum of **7** in CD_3CN also nicely demonstrates the difference in lability between axial and equatorial sites in such systems. The axial MeCN groups exchange rapidly with bulk solvent on the NMR time scale at room temperature and appear as free MeCN (1.95 ppm), while the equatorial MeCN ligands (2.24 ppm) are not exchanged under the same conditions after 7 days. This is in contrast to the equatorial MeOH in **4**, which exchanges relatively rapidly in MeOH solution.

Discussion

The described results establish that two distinct modes of bpy binding result from the reaction of 1 equiv of bpy with $Rh_2(O_2CR)_4L_2$ *viz.* an *ax-eq* (**3**) or an *eq-eq* (**4**, **5**, **7**) disposition of the bpy N-atoms. The identification of the former is important in a broader context as it may provide insight into the mechanism of attack of N-donor chelates on a dinuclear unit. As shown in Scheme I, the suggested sequence of events for this reaction system

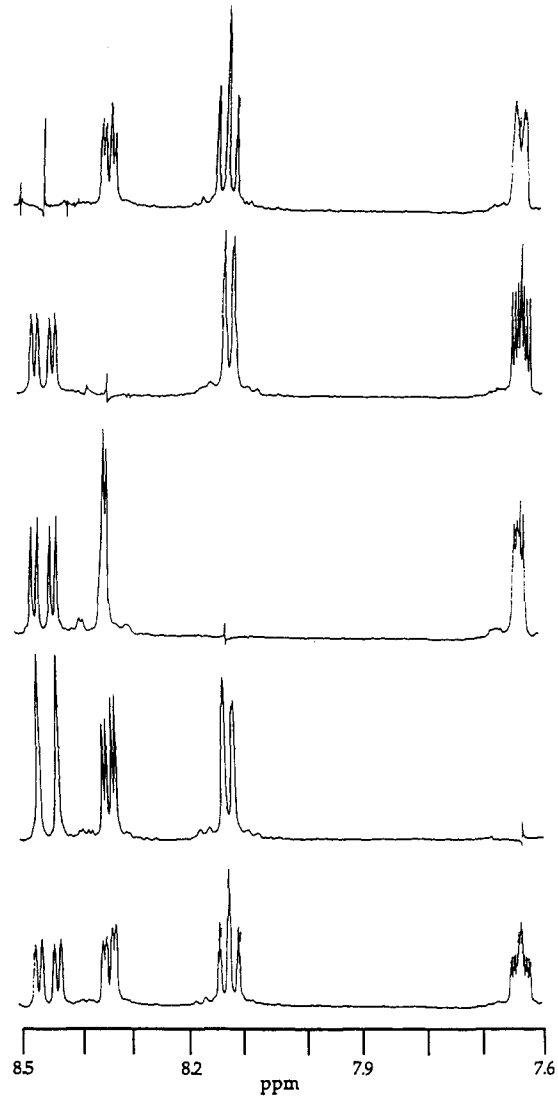

Figure 8. Spectra showing the results of selective homonuclear decoupling in the aromatic region for complex **4**.

is nucleophilic attack by the bpy at an axial site of $Rh_2(O_2CR)_4L_2$ (L = MeOH (**1**), Me_2CO (**2**)) to give an axially-bound monodentate bpy (step a), which then undergoes chelate ring formation by attack of the second bpy nitrogen at an equatorial site with displacement of an oxygen of a bridging RCO_2^- group (step b). The partially-displaced carboxylate then may adopt an *ax-eq* chelating mode thereby giving **3** (step c). In MeOH solution, the *ax-eq* bpy converts (step d) to an *eq-eq* mode, with one carboxylate then dissociating to give a salt (complex **4**) containing an equatorial MeOH (step e). In contrast, the CF_3COO^- reagent **2** reacts with bpy to give molecular complex **5**, i.e., *two* equatorial, monodentate groups. The CF_3COO^- reagent also gives a molecular species (**5'**) when the reaction is carried out in H_2O (or Me_2CO) suggesting that the identity of the isolated product (ionic *vs* molecular) is not simply a function of the solvent dielectric constant but is dependent on factors that likely include the identity of the carboxylate and preferential solubilities of species in equilibrium.

If the sequence of events depicted in Scheme I correctly describes the mechanism of attack of bpy on the $Rh_2(OAc)_4$ unit, no reaction should occur with N-chelates that cannot occupy an axial position due to steric reasons. To test this possibility, the bpy derivative 2,2'-biquinoline (bqn) was employed; models show that severe steric repulsions between the fused rings and the carboxylate groups should prevent the N atom from approaching and occupying the axial coordination sites. Indeed, treatment of an MeCN solution of $Rh_2(OAc)_4(MeOH)_2$ with bqn gave no reaction, even after 48 h at reflux, as confirmed by ^1H NMR (the

Pictiva EX2017
Samsung v Pictiva
IPR2024-01094

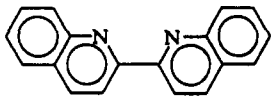

bqn

bqn precipitates from solution on cooling, allowing facile separation of reagents). It appears that the reaction is kinetically prevented (inability to undergo step a) since there is no obvious steric or other reason for the bqn analogue of **4** or **5** not to be the thermodynamically-preferred product, as in the corresponding bpy reactions. The absence of reaction with bqn is therefore considered to represent support for step a of the mechanism presented in Scheme I.

Support for step b and the formation of an *ax-eq* species is supported by the isolation of **3** and by the reaction of $Rh_2(OAc)_4(MeOH)_2$ with bpy in MeOH. The NMR spectra for the latter reaction clearly indicate the initial formation of a compound with NMR spectral features characteristic of an *ax-eq* species that then converts to the *eq-eq* product **4**. The intermediate species does not possess the *exact* structure of **3** (as gauged by NMR), nor should it be expected to do so in good donor solvents; i.e., a structure involving a monodentate, equatorial AcO^- and axial MeOH groups is more likely. The precipitation of **3** from the reaction in Me_2CO solution thus appears to be a case in which a metastable reaction intermediate has been trapped by precipitation. This also rationalizes the instability of **3** on redissolution, even in nondonor solvents such as CH_2Cl_2.

Biological Significance. In the Introduction, it was stated that the main goal of this work was to determine the products from the reaction of N-donor chelates with the dinuclear Rh carboxylate core and thus gain insights into feasible binding modes of the latter to DNA. The obtained results indicate that although initial binding is, as expected, at the axial sites, the ultimate, stable products contain equatorially-bound chelate groups. Thus, the displacement by the chelate of some of the carboxylate groups from equatorial positions readily occurs. While not wishing to draw definite conclusions from bpy reactions about what might or might not occur with DNA groups, we find the obtained results do allow some potentially useful insights to be gleaned. Certainly, we agree with previous assertions that DNA adenine groups bind

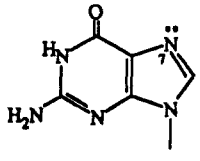

guanine

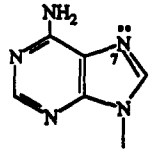

adenine

to the Rh_2^{4+} core at the axial positions employing the N(7) nitrogen lone pair; there are already many well-characterized examples of monodentate N-donor groups bound to these axial positions.[28] However, the results with bpy suggest that it is feasible that DNA sites possessing two adjacent purine bases might then trigger subsequent structural changes; i.e., binding of one purine N(7) to an axial site might then be followed by attack of the second N(7) at an equatorial site, initiating a sequence of events that could lead to both purine groups becoming coordinated at equatorial sites. This would be analogous to the bpy binding modes in **4**, **5**, and **7**. We note that the ~90° bite angle displayed by, for example, the d(pGpG) "chelate" ligand in the cisplatin adduct is admirably suited to also bind at two *cis* equatorial positions of one Rh atom in a dinuclear Rh carboxylate complex.[8,9]

Scheme I

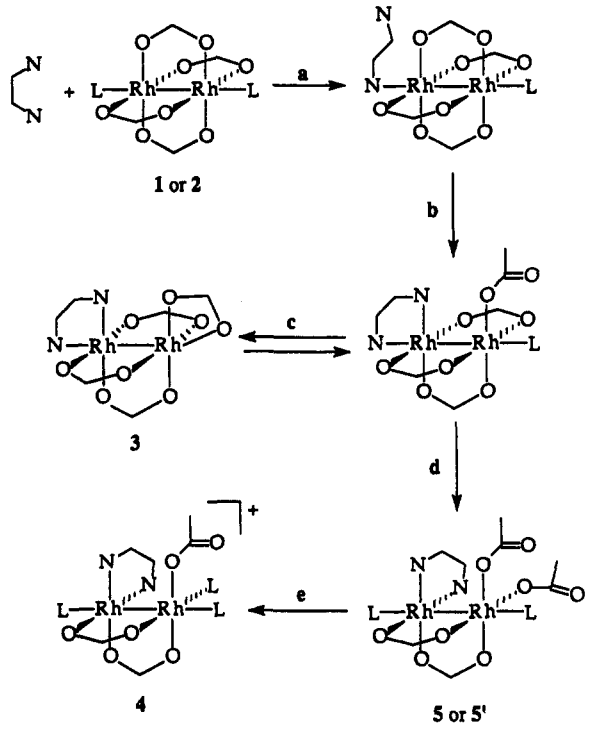

To answer one of the questions implied in the Introduction, we believe it is thus indeed a distinct possibility that dinuclear $Rh_2(O_2CR)_4$ complexes *could* bind to DNA in a fashion analogous to cisplatin *viz.* two adjacent purine bases. We also note that others have already commented on the fact that the necessarily-weak axial binding of purine rings to $Rh_2(O_2CR)_4$ is unlikely to be the basis of the observed carcinostatic activity.[1d] Again, the implication supported by the present work is that equatorial binding is involved.

It is important to remember at this point that, by themselves, adenines bind preferentially over guanines to the axial sites of $Rh_2(O_2CR)_4$ complexes, due to the NH···O hydrogen bonds mentioned in the Introduction. This, however, does not preclude subsequent binding by an *adjacent* base (adenine or guanine) at the equatorial positions. Conventional wisdom suggests that guanine groups do not bind to $Rh_2(O_2CR)_4$ complexes at all,[1,3,19] a matter that we are currently reinvestigating in detail.

We terminate this discussion at this point because it is clear that our attention must now turn to the use of DNA bases either by themselves or linked in a dinucleotide sequence. It is important to determine if and under what conditions adenine and/or guanine groups are capable of binding to the equatorial positions and, if they are, the precise structures of the resulting products. Such studies are, in fact, already well advanced, and these results will be reported in due course.

Acknowledgment. We thank Dr. S. P. Perlepes for his contributions to the initial stages of this work, S. N. Bernstein for assistance with the FAB Mass Spectrometry, and Dr. Feng Lin for assistance with ^1H NMR spectroscopy. This work was supported by NSF Grants CHE-8808019 (G.C.) and CHE-8914915 (K.R.D.). X-ray crystallography instrumentation was purchased with NSF Equipment Grants CHE-8908088 and CHE-9113668.

Supplementary Material Available: A textual presentation of the structure solution and tables of crystal data, fractional coordinates, thermal parameters, and bond distances and angles for complexes **3**, **5**, and **7** (32 pages). Ordering information is given on any current masthead page.

Pictiva EX2017
Samsung v Pictiva
IPR2024-01094